INTERNATIONAL JOURNAL OF AGRICULTURE & BIOLOGY
ISSN Print: 1560–8530; ISSN Online: 1814–9596
20F–056/202x/00–0–000–000
DOI: 10.17957/IJAB/15.1484
http://www.fspublishers.org

Full Length Article

Description of *Fusarium soli* Isolated from the Soil of a Poplar Plantation in China

Yun-Jia Zhu, Xing-Ye Yu, Bao-Teng Wang, Long Jin* and Feng-Jie Jin*
College of Biology and the Environment, Co-Innovation Centre for Sustainable Forestry in Southern China, Nanjing Forestry University, Nanjing 210037, China
*For correspondence: isacckim@kaist.ac.kr; jinfj@njfu.edu.cn
Received 06 March 2020; Accepted 20 April 2020; Published _____

Abstract

A novel filamentous fungus was isolated from the upper layer of soil in a poplar plantation of Jiangsu Province in eastern China. Morphological observations showed that the strain exhibited typical sickle-shaped and multicellular macroconidia. In addition, the strain was also found to produce microconidia and chlamydospores on the surface of mycelia under different culture conditions. These results and further phenotypic observations revealed that the morphological characteristics of this isolated fungus were extremely similar to those of fungi in the genus *Fusarium*. Moreover, the phylogenetic analysis based on *EF-1α*, *RPB1*, *RPB2* and LSU genes indicated that the strain had the highest similarity (99.28, 97.89, 99.43 and 81.17%) to *Fusarium convolutans* for *EF-1α*, *RPB1*, *RPB2* and LSU, respectively. Based on the phylogenetic relationships together with physiological characteristics, we proposed that strain PD2^T represents a novel species of the genus *Fusarium*, and the name *F. soli* sp. nov. is proposed. The type strain is PD2^T. © 2020 Friends Science Publishers

Key words: *Fusarium*; Macroconidia; Morphology; Phylogeny; Soil

Introduction

Fusarium is a large genus of filamentous fungi that is widely distributed in soil, plants and animals. This fungal genus is one of the most important plant pathogens and can cause a variety of plant diseases (Bai *et al.* 2002; Dean *et al.* 2012; Coleman 2016), thereby affecting the growth of crops and other plants and reducing their economic value. In addition, it also harbors mycotoxin producers that can produce several extremely important mycotoxins, such as trichothecenes and fumonisins (Ilgen *et al.* 2008; Woloshuk and Shim 2013), and opportunistic human pathogens (Desjardins 2006; Tupaki-Sreepurna *et al.* 2018). Although *Fusarium* species are of great economic importance because of their beneficial and harmful effects, they are difficult to identify.

In 1809, the genus *Fusarium*, with *Fusarium roseum* as the model species, was first described by Link, Heinrich Friedrich. In 1935, the first complete taxonomic system of *Fusarium* was proposed, and it divided *Fusarium* into 16 groups and 65 species and became the basis for the taxonomic study of *Fusarium* (Wollenweber and Reinking 1935). From 1945 to 1983, scholars have proposed 10 different classification systems (Snyder and Hansen 1940; Booth 1971; Gerlach and Nirenberg 1982; Nelson *et al.* 1983), and the most influential system was proposed by Nelson *et al.* (1983). To date, more than 300 different *Fusarium* species have been discovered, and nearly half have not been formally described (O'Donnell *et al.* 2018; Summerell 2019). Nevertheless, some *Fusarium* species have been isolated, identified and characterized, such as *F. oxysporum*, which could cause a variety of root-rot diseases (Pérez-Hernández *et al.* 2014; Liu *et al.* 2016); and *F. graminearum*, which could lead to head blight of wheat (Duan *et al.* 2019; Rojas *et al.* 2020). Most plant species have one or more fusarium diseases that affect their production. *Fusarium* spp. have both the asexual and sexual states in their life cycles. In morphological taxonomy, some morphological characteristics could provide a useful reference for the identification of *Fusarium* spp. such as the presence of the typical banana-shaped macroconidia, chlamydospores formed from hyphae, as well as microconidia and sexual reproductive structures. However, because the morphology of *Fusarium* spp. is complex and susceptible to environmental impacts, results based on morphological characteristics are not very accurate. Currently, molecular classification techniques, such as DNA markers to distinguish species and molecular phylogenetic analyses, have been successfully applied to the identification of the species of genus *Fusarium*.

In this study, soil samples were collected from a poplar plantation (32°52'28.45''N, 120°49'47.63''E) located in Jiangsu Province, Eastern China. The poplar

plantation is close to the Yellow Sea State Forest Park and belongs to the transition region between the subtropics and warm-temperate zones. It has obvious transitional, oceanic and monsoon climates. The soil is classified as a Fluvisol according to the World Reference Base (WRB), and the soil pH is alkaline. From these collected soil samples, some interesting filamentous fungi were isolated. According to the morphological characteristics and molecular identification, a new species of the genus *Fusarium* is identified and described in this paper.

Materials and Methods

Isolation and culture condition

Soil samples were collected from the Dongtai Poplar Plantation (32°52'28.45''N, 120°49'47.63''E) of Jiangsu Province in eastern China. The soil had a sandy texture and was alkaline, and no fertilization or other treatments were conducted. Martin's plate (10 g of dextrose, 5 g of peptone, 0.5 g of $MgSO_4 \cdot 7H_2O$, 1 g of KH_2PO_4, 3.3 mL of 0.1% Bengal Red Solution, 20 g of agar, 3.3 mL of 1000 UmL^{-1} streptomycin solution, 20 mL of 2% sodium deoxycholate solution and 1 L of water) was used as the fungal isolation medium. Subsequently, 0.5 g soil samples were diluted along a gradient (10^{-1}, 10^{-2}, 10^{-3}, 10^{-4}, 10^{-5}) with sterile distilled water and then coated on the fungi isolation medium. After 3–10 days of incubation at 30ºC, single colonies were selected for further isolation and purification.

Morphological, physiological, and biochemical characterization

The isolated strain was cultivated on synthetic low nutrient agar (SNA; Elite-Media, China), Potato dextrose agar (PDA; BD Difco, Sparks, M.D., U.S.A.) and Czapek yeast agar (CYA; Kalang, Shanghai, China) and incubated at 30ºC for 7 days to obtain colony growth. The morphology of the strain was observed during this period. The strain was cultured on a VBC plate (0.5 g of dextrose, 1 g of KH_2PO_4, 1 g of $NaNO_3$, vitamin B, vitamin C, 20 g of agar, and 1 L of water) (Wang and Chen 1994) and incubated in a constant temperature incubator at 30ºC for 7 days. Spore production was observed during incubation. An inverted microscope (IX73, Olympus, Tokyo, Japan) was used for microscopic observation, and an advanced scientific camera control (Digital Optics, Ltd., Auckland, New Zealand) equipped with OCULAR software (Digital Optics, Ltd.) was used for image analysis.

Growth temperature of the strain: The strain was grown at different temperatures (4, 15, 25, 30 and 35ºC), and PDA (BD Difco) was used to investigate the temperature range of strain growth. Growth was observed during culturing at different temperatures for 7 days.

The carbon source utilization of the strain was investigated by using the carbon source identification plate FF Micro Plate™ (Biolog Inc., Hayward, CA, USA).

Molecular characterization

The high-fidelity PCR enzyme KOD FX DNA Polymerase (TOYOBO, Osaka, Japan) was used to amplify the target genes from the fungal mycelia directly. The translation elongation factor 1-alpha gene (*EF-1α*), the largest subunit of the RNA polymerase gene (*RPB1*), the sec largest subunit of the RNA polymerase gene (*RPB2*) and 28 S large subunit (LSU) sequences were amplified in a Gene Amp 9700 system (Applied Biosystems, Foster City, CA, USA) with primer pairs EF1/EF2 (O'Donnell *et al.* 2008), Fa/G2R (O'Donnell *et al.* 2010), 5F2/7cR (O'Donnell *et al.* 2007), and NL1/NL4 (Kwiatkowski *et al.* 2012). The PCRs were performed as follows: initial denaturation at 94ºC for 4 min; followed by 40 cycles at 98ºC for 10 s, 50ºC for 30 s, and 68ºC for 30 s; and a final extension at 72ºC for 7 min. The PCR products were isolated using agarose gel electrophoresis and then purified using a TaKaRa MiniBEST DNA Fragment Purification Kit (TaKaRa, Otsu, Japan). The purified PCR products were further sequenced and analyzed. The DNA sequence data were deposited in GenBank under accession numbers MN848239, MN848237, MN848238 and MN809346. Previously published sequences included in this study are available from the GenBank database (Table 1).

DNA sequences were aligned with ClustalX (Thompson *et al.* 1997), and then edited and trimmed by using BioEdit software (Hall 1999). The *EF-1α*, *RPB1*, *RPB2* and LSU sequences of the strain isolated in this study and similar model strains were used to construct the phylogenetic tree by using the Neighbor-joining method (Saitou and Nei 1987) in MEGA 5.0 software (Tamura *et al.* 2011). The evolutionary distances were computed using the Kimura 2-parameter method (Kimura 1980), and the unit is the number of base substitutions per site. Gaps and missing data were taken into consideration when > 95% unambiguity was encountered. One thousand bootstrap methods were used (Felsenstein 1985).

Results

Morphological, physiological and biochemical characteristics

The strain $PD2^T$ isolated from a soil sample was spot-cultured on PDA, SNA, and CYA plates at 30℃ for 7 days to obtain colony growth and observe the morphology of the strain (Table 1). The diameter of a 7-day old single colony on PDA medium was 67-73 mm, on CYA medium was 85-86 mm, and on SNA medium was 48–53 mm. On PDA medium, the edge of the colony was light brown and irregular, the aerial hyphae were white, the spores were transparent to white, and the reverse colony was light orange. On CYA medium, the surface of the colony was wrinkled, the aerial hyphae were white, the spores were transparent to white, and the reverse colony was light yellow. On the SNA

Table1: Strains used in the molecular phylogenetic analysis in this study

Species	Source	Substrate/Host	Origin	GenBank accession number					Reference
				EF-1α	RPB1	RPB2	LSU	ITS	
PD2	—	Soil	China	MN848239	MN848237	MN848238	MN809346	MN559538	In this study
Fusarium convolutans	CBS 144207^T	*Kyphocarpa angustifolia* rhizosphere	South Africa	LT996094	LT996193	LT996141	MN749523	—	Sandoval-Denis *et al.* (2018)
F. sublunatum	CBS 189.34^T=BBA 62431^T	Soil of banana plantation	Costa Rica	—	JX171451	JX171565	KM231680	NR111606	Nelson *et al.* (1983); Gräfenhan *et al.* (2011); Lombard *et al.* (2015)
	NRRL 20897	Unknown	Unknown	KX302919	KX302927	KX302935	—	—	—
F. algeriense	NRRL 66647^T	Durum, wheat	Algeria	MF120510	MF120488	MF120499	—	NR158423	Laraba *et al* (2017)
F. concolor	NRRL 13994^T	*Hordeum vulgare*	Uruguay	MH742650	MH742492	MH742569	—	—	Jacobs-Venter *et al.* (2018)
F. beomiforme	NRRL 13606^T	Soil	Australia	MF120507	MF120485	MF120496	U34553	—	Laraba *et al.* (2017)
F. coffeatum	CBS 635.76^T	*Cynodonlemfuensis*	South Africa	MN120755	MN120717	MN120736	NG057718	—	Lombard *et al.* (2019)
F. napiforme	NRRL 13604^T	*Pennisetumtyphoides*	Namibia	AF160266	HM347136	EF470117	U34541	—	Nirenberg and O'Donnell (1998)
F. inflexum	NRRL 20433^T=CBS 716.74^T	*Viciafaba* vascular bundle, wilting plant	Germany	AF008479	JX171469	JX171583	U34548	—	O'Donnell *et al.* (1998)
F. globosum	NRRL 26131^T	*Zea mays*	South Africa	KF466417	KF466396	KF466406	AY249384	—	Proctor *et al.* (2013)
F. petersiae	CBS 143231^T	Garden soil	Netherlands	MG386159	MG386138	MG386149	NG058528	NR156397	Crous *et al.* (2017)
F. ananatum	CBS 118516^T	*Ananas comosus* fruit	South Africa	LT996091	LT996188	LT996137	KU604065	—	Sandoval-Denis *et al.* (2018)
F. transvaalense	CBS 144211^T	*Sidacordifolia* rhizosphere	South Africa	LT996099	LT996210	LT996157	—	—	Sandoval-Denis *et al.* (2018)
F. concentricum	CBS 450.97^T	*Musa sapientum* fruit	Costa Rica	AF160282	LT996192	LT575063	U61652	—	Nirenberg and O'Donnell (1998)
F. bulbicola	CBS 220.76^T = NRRL 13618^T	*Nerine bowdenii*	Germany	KF466415	KF466394	KF466404	U61650	—	Proctor *et al.* (2013)
F. babinda	CBS 397.96^T	Soil in *Nothofagus* forest	Victoria	—	—	—	MH874204	NR159861	O'Donnell *et al.* (2013, 2015)
F. domesticum	CBS 434.34^T	Cheese	Belgium	—	—	—	NG057952	NR145050	Bachmann *et al* .(2005); Ropars *et al.* (2012)
F. penzigii	CBS 317.34^T	*Fagus sylvatica* decayed wood	England	EU926324	KM232211	KM232362	KM231661	NR137707	Schroers *et al.* (2009)
F. nurragi	CBS 393.96^T	Soil in heath land	Victoria	—	—	—	—	NR159860	O'Donnell *et al.* (2013)
F. biseptatum	CBS 110311^T	Ex soil	South Africa,Transkei	—	—	—	—	NR137706	Schroers *et al.* (2009)
Fusicolla acetilerea	IMI 181488^T	Polluted soil	Japan	—	—	—	—	NR111603	Tubaki *et al.* (1976)
F. violacea	NRRL 20896^T	*Quadraspidiotusperniciosus* on dying twig of *Prunus domestica*	Iran	—	—	—	—	NR137617	Gräfenhan *et al.* (2011)
Neonectria lugdunensis	CBS 250.58^T	*Ilex aquifolium* submerged decaying leaf	U.K.	—	—	—	—	NR155466	Chaverri *et al.* (2011)
N. major	CBS 240.29^T	Canker on *Alnusincana*	Norway	—	—	—	—	NR121496	Chaverri *et al.* (2011)
Paracremonium inflatum	CBS 485.77^T	Man	India	—	—	—	—	NR154312	Lombard *et al.* (2015)
P. binnewijzendii	CBS 143277^T	Soil	Netherlands	—	—	—	—	NR157491	Crous *et al.* (2017)
Pseudocosmos poraeutypellae	CBS 133966^T	*Eutypella* sp.	USA,Maryland, Beltsville	—	—	—	—	NR158888	Herrera *et al.* (2013)
P. porametajoca	BPI 879088^T	*Eutypa* sp.	New Zealand	—	—	—	—	NR155633	Herrera *et al.* (2013)
P. porarogersonii	BPI 1107121^T	*Eutypella* sp.	U.S.A.	—	—	—	—	NR154295	Herrera *et al.* (2013)
Rectifusarium robinianum	NRRL 25729^T	*Robiniapseudoacacia* twig	Germany	—	—	—	—	NR154410	Lombard *et al.* (2015)

medium, the positive and negative sides of the colony were white and translucent, the aerial hyphae were white, and the spores were transparent to white (Fig. 1 a–c).

The morphological structure of the strain was further observed by microscopy (Fig. 1 d–m). Microconidia were columnar; macroconidia were moderate in number, sickle-shaped, and segregated and most had 3–6 septate; the sporogenesis cell type was single-bottle-stalk sporogenesis; the conidia stalk was lateral; the chlamydospore was spherical, single or catenulate and showed intercalary and clustered growth and a high quantity. Sclerotial bodies were not observed. These morphological characteristics, especially the typical sickle-shaped and multicellular macroconidia as well as the spherical intercalary chlamydospores are very similar to those of *Fusarium* species, suggesting that this new isolate PD2^T may be a member of the genus *Fusarium*. The growth temperature of the strain PD2^T was investigated by cultivation on PDA plates at different temperatures (4, 15, 25, 30 and 35ºC) for 7 days. The results indicated that the temperature range of the strain growth on PDA medium is 15–30ºC.

Furthermore, the carbon source utilization of the strain was examined using the Biolog FF Micro Plate. After 48 h of incubation on the carbon source identification plate, the available carbon sources of the isolate were as follows: i-erythritol, glucose-1-phosphate, glycerol, γ-hydroxy-butyric Acid, *p*-hydroxyphenyl acetic acid, α-keto-glutaric acid, D-saccharicacid, L-alanine, L-alanyl-glycine, L-asparagine, L-aspartic acid, L-glutamic acid, L-ornithine, L-phenylalanine, L-serine, L-threonine, and adenosine-5'-monophosphate (Table 2).

Phylogenetic analyses

The sequences of *EF-1α*, *RPB1*, *RPB2* and LSU genes of the isolate PD2^T were subjected to a BLAST sequence alignment on the NCBI website, and the results showed that the genus *Fusarium* had the highest similarity with this strain. Some sequences from the alignment results were selected to construct phylogenetic trees. The strains used in the molecular phylogenetic study are listed in Table 1. To analyze the phylogenetic relationship, we selected the following strains and used them for phylogenetic tree construction: the new isolate and 14 *Fusarium* species belonging to the *F. buharicum* (FBSC), *F. fujikuroi* (FFSC), *F. tricinctum* (FTSC), *F. sambucinum* (FSAMSC), *F. incarnatum-equiseti* (FIESC), *F. oxysporum* (FOSC), *F. burgessii* and *F. concolor* species complexes (Fig. 2). According to the phylogenetic tree, the new isolate can be clustered within the FBSC clade (Vu *et al.* 2018) based on the combined sequences of partial *EF-1α*, *RPB1* and *RPB2* genes (Fig. 2). In addition to strain PD2^T, *F. convolutans* (CBS 144207) and *F. sublunatum* (CBS 189.34) are also clustered in the FBSC clade. The similarity analysis of the combined sequences (partial sequences of *EF-1α*, *RPB1* and *RPB2* genes) showed that the PD2^{T}strain had the highest sequence similarity of 98.89% with *F. convolutans*, followed by *F. sublunatum* (94.18%). Despite the high sequence similarity (99.28%, 97.89% and 99.43% identical to *F. convolutans* for *EF-1α*, *RPB1*, and *RPB2*), a further BLAST analysis indicated that the LSU sequence of the PD2^T strain is 81.17% identical to that of *F. convolutans*, implying that the PD2^T strain may not belong to *F. convolutans*.

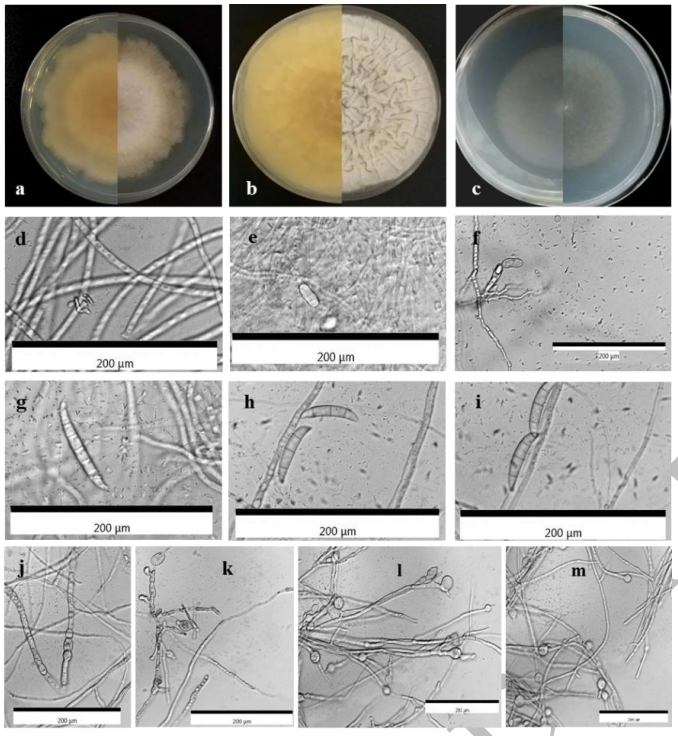

Fig. 1: *Fusarium soli* (PD2^T). **a-c**. Colony morphology grown on PDA, CYA, and SNA after 7 days at 30 ºC in the dark. **d-e**. Phialides and microconidia on PDA. **f**. Phialides and microconidia on CD. **g**. Macroconidia on SNA. **h-i**. Macroconidia on VBC. **j-k**. Chlamydospores on CYA. **l-m**. Chlamydospores on PDA

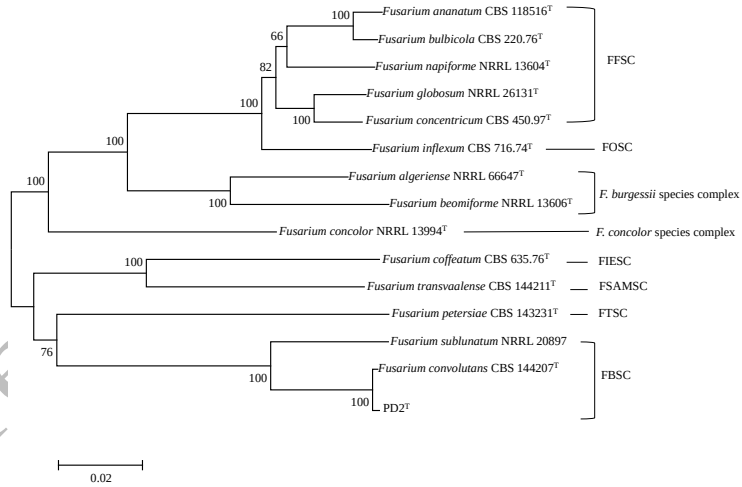

Fig. 2: Phylogenetic tree based on the sequences combined with the *EF-1α*, *RPB1* and *RPB2* genes of 15 strains. The evolutionary history was inferred using the neighbour-joining method in MEGA software version 5. Bars, 0.02 expected nucleotide substitutions per site. Only bootstrap values above 50 % are shown (1000 replicates) at branching points. The strains used here belong to *F. buharicum* (FBSC), *F. fujikuroi* (FFSC), *F. tricinctum* (FTSC), *F. sambucinum* (FSAMSC), *F. incarnatum-equiseti* (FIESC), *F. oxysporum* (FOSC), *F. burgessii* and *F. concolor* species complexes

To further study the phylogenetic relationship of the isolate and other *Fusarium* species, the phylogenetic tree was generated based on a combination of partial sequences, including *EF-1α* and LSU (Fig. 3). Twelve strains were selected for further construction and analysis of a phylogenetic tree, and the results showed that the new isolate PD2^T is distributed in the FBSC clade while the other 11 species belong to the FBSC, FFSC, FTSC, FIESC, FOSC, *F. dimerum* (FDSC) and *F. burgessii* species complexes. The *EF-1α* plus LSU sequence similarity of the new isolate PD2^T is 96.36% identical to that of *F. convolutans* (Fig. 3).

Another phylogenetic tree constructed using the

Table 2: Carbon source utilization of the species

Carbon source	Reaction	Carbon source	Reaction	Carbon source	Reaction
Water	—	Lactulose	—	γ-Hydroxy-butyric Acid	+++
Tween 80	+	Maltitol	—	p-Hydroxyphenylacetic Acid	++
N-Acetyl-D-galactosamine	—	Maltose	—	α-Keto-glutaric Acid	++
N-Acetyl-D-glucosamine	—	Maltotriose	—	D-Lactic Acid Methyl Ester	—
N-Acetyl-D-mannosamine	—	D-Mannitol	+	L-Lactic Acid	—
Adonitol	—	D-Mannose	—	D-Malic Acid	+
Amygdalin	—	D-Melezitose	—	L-Malic Acid	+
D-Arabinose	—	D-Melibiose	—	Quinic Acid	+
L-Arabinose	—	α-Methyl-D-galactoside	—	D-Saccharic Acid	+++
D-Arabitol	+	β-Methyl-D-galactoside	+	Sebacic Acid	—
Arbutin	+	α-Methyl-D-glucoside	—	Succinamic Acid	—
D-Cellobiose	—	β-Methyl-D-glucoside	—	Succinic Acid	++
α-Cyclodextrin	—	Palatinose	—	Succinic Acid Mono-mMethyl Ester	—
β-Cyclodextrin	—	D-Psicose	—	N-Acetyl-L-glutamic Acid	—
Dextrin	+	D-Raffinose	—	Alaninamide	+
i-Erythritol	++	L-Rhamnose	—	L-Alanine	+++
D-Fructose	—	D-Ribose	—	L-Alanyl-glycine	+++
L-Fucose	—	Salicin	+	L-Asparagine	+++
D-Galactose	—	Sedoheptulosan	—	L-Aspartic Acid	++
D-Galacturonic Acid	—	D-Sorbitol	+	L-Glutamic Acid	++
Gentiobiose	—	L-Sorbose	+	Glycyl-L-glutamic Acid	+
D-Gluconic Acid	—	Stachyose	+	L-Ornithine	+++
D-Glucosamine	—	Sucrose	—	L-Phenylalanine	+++
α-D-Glucose	—	D-Tagatose	—	L-Proline	—
Glucose-1-phosphate	+++	D-Trehalose	—	L-Pyroglutamic Acid	—
Glucuronamide	—	Turanose	—	L-Serine	+++
D-Glucuronic Acid	+	Xylitol	—	L-Threonine	+++
Glycerol	+++	D-Xylose	—	2-Amino Ethanol	—
Glycogen	+	γ-Amino-butyric Acid	—	Putrescine	—
m-Inositol	—	Bromosuccinic Acid	—	Adenosine	—
2-Keto-D-gluconic Acid	—	Fumaric Acid	—	Uridine	—
α-D-Lactose	—	β-Hydroxy-butyric Acid	—	Adenosine-5'-Monophosphate	+++

Growth reactions: —, no growth; +, weak growth; ++, moderate growth; +++, strong growth

combined partial sequences of *RPB1*, *RPB2* and LSU genes (Fig. 4) also showed that the strain PD2^T is still clustered in the FBSC clade. The combined sequence of *RPB1*, *RPB2* and LSU genes shared 97.54% and 94.22% similarity with those of *F. convolutans* and *F. sublunatum*, respectively. In addition to these two strains, the DNA sequences of other *Fusarium* species showed less similarity with this strain. Overall, these molecular phylogenetic analyses of the above mentioned genes demonstrated that this new discovered strain PD2^T is a new species distributed in the FBSC, and it is named *Fusarium soli* spp. nov.

Description of *Fusarium soli* spp. nov

***F. soli* spp. nov:** The temperature range for strain growth on PDA medium is 15–30°C. On PDA, the diameter of a single colony was 67–73 mm after 7 days at 30°C, the edge of the colony was light brown, the aerial hyphae were white, the spores were transparent to white, and the reverse colony was light orange. On CYA, the diameter of a single colony was 85–86 mm after 7 days at 30°C, the surface of the colony was wrinkled, the aerial hyphae were white, the spores were transparent to white, and the reverse colony was light yellow. On SNA, the diameter of a single colony was 48–53 mm after 7 days at 30°C, the positive and negative sides of the colony were white and translucent, the aerial hyphae were white, and the spores were transparent to white. Microconidia were columnar; macroconidia were moderate in number, sickle-shaped, and segregated and most had 3–6 septate; the sporogenesis cell type was single-bottle-stalk; the conidia stalk was lateral; the chlamydospore was spherical, single or catenulate and showed intercalary and clustered growth and a high quantity.

The type strain PD2^T was isolated from the upper layer of soil in a poplar plantation (32°52’28.45’’N, 120°49’47.63’’E) of Jiangsu Province in eastern China.

Discussion

The new species described in this paper was identified to belong to the genus *Fusarium* based on the presence of typical morphological features, such assickle-shaped macroconidia and intercalary chlamydospores. In the study by O’Donnell (2015), *EF-1α*, *RPB1* and *RPB2* genes could be used for the accurate identification of the genus *Fusarium*. According to the phylogenetic trees (Fig. 2–4), the strain PD2^T has the closest relationship with *F. convolutans* (Sandoval-Denis *et al.* 2018). The minimum and maximum temperatures for growth of this strain on PDA are 12°C and 36°C, respectively. The surface of the colony is white to cream colored, with short aerial mycelium; and the margin of colony is irregular to rhizoid,

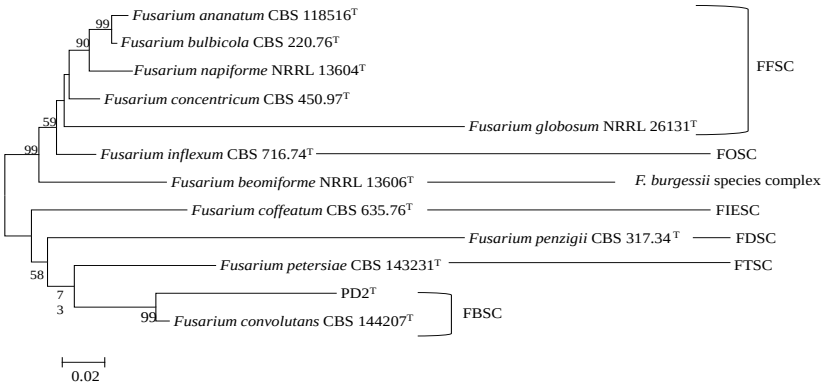

Fig. 3: Neighbour-joining phylogenetic tree based on the sequences combined with the *EF-1α* and LSU genes of 12 strains. Bars, 0.02 expected nucleotide substitutions per site. Only bootstrap values above 50% are shown (1000 replicates) at branching points. The strains used here belong to *F. buharicum* (FBSC), *F. fujikuroi* (FFSC), *F. tricinctum* (FTSC), *F. incarnatum-equiseti* (FIESC), *F. oxysporum* (FOSC), *F. dimerum* (FDSC) and *F. burgessii* species complexes.

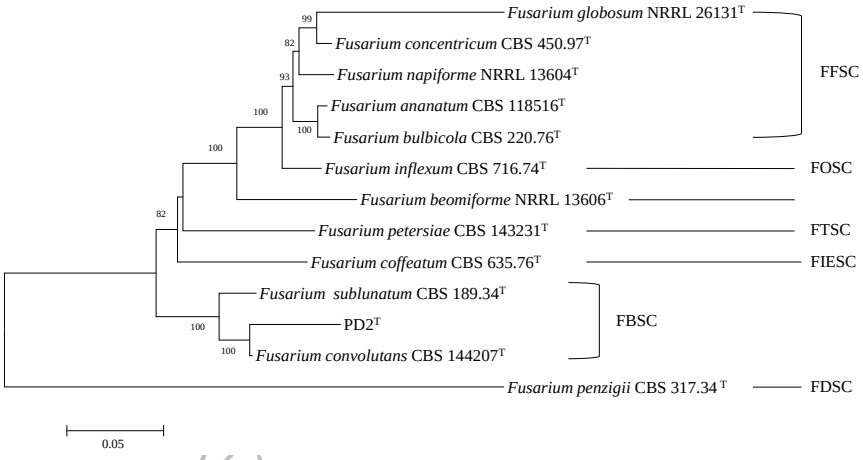

Fig. 4: Neighbour-joining phylogenetic tree based on the sequences combined with the *RPB1*, *RPB2* and LSU genes of 13 strains. Bars, 0.05 expected nucleotide substitutions per site. Only bootstrap values above 50% are shown (1000 replicates) at branching points. The strains used here belong to *F. buharicum* (FBSC), *F. fujikuroi* (FFSC), *F. tricinctum* (FTSC), *F. incarnatum-equiseti* (FIESC), *F. oxysporum* (FOSC), *F. dimerum* (FDSC) and *F. burgessii* species complexes

with abundant white to gray submerged mycelium. The reverse side is white with straw to yellow diffusible pigment. Sporulation is scant from conidiophores formed on aerial mycelia, and sporodochia are not observed. Conidiophores on the aerial mycelia are straight or curved, smooth and thin-walled, and simple, and most of them degenerate into conidia cells; phialides are subulate to subcylindrical, and smooth- and thin-walled; and the conidia are lunate to falcate shaped and curved or somewhat straight, with (1–2–)3-septa. Chlamydospores are abundant, globose to sub globose, terminal or intercalary in the hyphae or conidia, and they are often borne laterally at the tip of elongated, cylindrical, stalk-like projections and found alone or in small clusters.

Although the morphological characteristics of the strain *F. convolutans* are partially similar to those of the new isolate *F. soli*, some distinct characteristics can be used to distinguish them from each other. For example, compared with *F. convolutans*, the new isolate *F. soli* has more sparse aerial hyphae on SNA, up to 6-septate macroconidia, catenulate chlamydospores and no curved sterile hypha. In addition, under the same culture conditions, the strain *F. soli* has a significantly faster growth rate than the strain *F. convolutans*. These different morphological characteristics combined with the molecular phylogenetic analysis results suggest that this isolate was a completely different species from *F. convolutans.*

The phylogenetic trees showed that in addition to the new isolate and *F. convolutans*, the strain *F. sublunatum* also belongs to the same FBSC clan. The aerial mycelia of

F. sublunatum are sparse and white; the sporodochia are orange; the sclerotia are dark blue to blue-green; microconidia are rare; the macroconidia are sickle-shaped with a distinctly foot-shaped basal cell; and the chlamydospores are abundant (Nelson *et al.* 1983; Gräfenhan *et al.* 2011; Lombard *et al.* 2015). *F. sublunatum* was also isolated from the soil and the perfect state is still unknown. However, according to the phylogenetic trees and BLAST analysis, *F. sublunatum* has only a relatively low sequence similarity with the isolate *F. soli*, and the new isolate can be distinguished from *F. sublunatum* by transparent to white sporodochia and the lack of sclerotia.

F. petersiae (CBS 143231) (Crous *et al.* 2017) is another strain of the genus *Fusarium* with relative lower sequence similarity to PD2^T based on the phylogenetic tree analysis. The morphological characteristics of *F. petersiae* on SNA included hyphae that were hyaline and smooth and absent chlamydospores; sporulation was abundant only from sporodochia; no conidiophores were observed on the aerial mycelia; sporodochia were abundant only on the surface of carnation leaves; macroconidia were falcate and curved and showed a papillate and curved apical cell that tapered towards a foot-like basal cell. *F. petersiae* is a new member of the *F. tricinctum* species complex (FTSC) that is closely related to *F. flocciferum* (Booth 1971) and *F. torulosum.* There are obvious differences in the morphological characteristics between *F. petersiae* and the new isolate PD2^T.

Combining the results of the molecular phylogenetic analyses and morphological characteristics indicates that the strain *F. soli* isolated in this study is a new species clustered in the FBSC of the genus *Fusarium.*

Conclusion

The new isolate showed the closest relationship with *F. convolutans* which was clustered in the FBSC clade. However, sequence similarity analyses combined with different morphological characteristics, such as macroconidia with more septa, catenulate chlamydospores and no curved sterile hypha, demonstrated that the isolate is a new species of the genus *Fusarium.* The carbon source utilization of the new isolate *Fusarium soli* was further examined in this study.

Acknowledgements

This study was supported by the Natural Science Foundation of China (31570107), the Six Talent Peaks Program of Jiangsu Province of China (TD-XYDXX-006) and Priority Academic Program Development of Jiangsu Higher Education Institutions (PAPD).

Author Contributions

The main author of this work, Y.-J.Z.; design of experiments, L.J. and F.-J.J.; original draft preparation and references investigation, Y.-J.Z., X.-Y.Y. and B.-T.W.; review and editing, L.J. and F.-J.J. All authors have read and agreed to the published version of the manuscript.

References

Bachmann HP, C Bobst, U Bütikofer, MG Casey, MD Torre, MT Fröhlich-Wyder, M Fürst (2005). Occurrence and significance of *Fusarium domesticum* alias Anticollanti on smear-ripened cheeses. *Food Sci Technol* 38:399–407

Bai GH, AE Desjardins, RD Plattner (2002). Deoxynivalenol-nonproducing *Fusarium graminearum* causes initial infection, but does not cause disease spread in wheat spikes. *Mycopathologia* 153:91–98

Booth C (1971). *The genus Fusarium*, pp: 1–237. Commonwealth Mycological Institute, Kew, UK

Chaverri P, C Salgado, Y Hirooka, AY Rossman, GJ Samuels (2011). Delimitation of *Neonectria* and *Cylindrocarpon* (Nectriaceae, Hypocreales, Ascomycota) and related genera with *Cylindrocarpon*-like anamorphs. *Stud Mycol* 68:57–78

Coleman JJ (2016). The *Fusarium solani* species complex: ubiquitous pathogens of agricultural importance. *Mol Plant Pathol* 17:146–158

Crous PW, L Lombard, JZ Groenewaldet (2017). Fungal Planet description sheets. *Persoonia* 39:270–467

Dean R, JAV Kan, ZA Pretorius, KE Hammond-Kosack, AD Pietro, PD Spanu, JJ Rudd, M Dickman, R Kahmann, J Ellis, GD Foster (2012). The top 10 fungal pathogens in molecular plant pathology. *Mol Plant Pathol* 13:414–430

Desjardins AE (2006). *Fusarium Mycotoxins: Chemistry, Genetics and Biology*. American Phytopathological Society, St. Paul, Minnesota, USA

Duan Y, X Tao, H Zhao, X Xiao, M Li, J Wang, M Zhou (2019). Activity of demethylation inhibitor fungicide metconazole on Chinese *Fusarium graminearum* species complex and its application in carbendazim-resistance management of Fusarium head blight in wheat. *Plant Dis* 103:929–937

Felsenstein J (1985). Confidence limits on phylogenies: An approach using the bootstrap. *Evolution* 39:783–791

Gerlach W, HI Nirenberg (1982). *The genus Fusarium - a pictorial atlas*, pp: 1–406. Berlin-Dahlem (Heft 209): Mitteilungenaus der Biologis-chenBundesanstaltfür Land-und Forstwirtschaft, Berlin, Germany

Gräfenhan T, HJ Schroers, HI Nirenberg, KA Seifert (2011). An overview of the taxonomy, phylogeny, and typification of nectriaceous fungi in *Cosmospora, Acremonium, Fusarium, Stilbella* and *Volutella*. *Stud Mycol* 68:79–113

Hall BG (1999). BioEdit: A user-friendly biological sequence alignment editor and analysis program for windows 95/98/NT. *In: Nucleic Acids Symposium Series*, Vol. 41, pp: 95–98. Information Retrieval Ltd., Oxford University, UK

Herrera CS, AY Rossman, GJ Samuels, P Chaverri (2013). *Pseudocosmospora*, a new genus to accommodate *Cosmosporavilior* and related species. *Mycologia* 105:1287–1305

Ilgen P, F Maier, W Sch¨afer (2008). Trichothecenes and lipases are host-induced and secreted virulence factors of *Fusarium graminearum*. *Cereal Res Commun* 36:421–428

Jacobs-Venter A, I Laraba, DM Geiser, M Busman, MM Vaughan, RH Proctor, SP McCormick, K O'Donnell (2018). Molecular systematics of two sister clades, the *Fusarium concolor* and *F. babinda* species complexes, and the discovery of a novel microcycle macroconidium–producing species from South Africa. *Mycologia* 110:1189–1204

Kimura M (1980). A simple method for estimating evolutionary rate of base substitutions through comparative studies of nucleotide sequences. *J Mol Evol* 16:111–120

Kwiatkowski NP, WM Babiker, WG Merz, KC Carroll, SX Zhang (2012). Evaluation of nucleic acid sequencing of the D1/D2 region of the large subunit of the 28S rDNA and the internal transcribed spacer region using SmartGene IDNS software for identification of filamentous fungi in a clinical laboratory. *J Mol Diagn* 14:393–401

Laraba I, A Keddad, H Boureghda, N Abdallah, MM Vaughan, RH Proctor, M Busman, K O'Donnell (2017). *Fusarium algeriense*, sp. nov., a novel toxigenic crown rot pathogen of durum wheat from Algeria is nested in the *Fusarium burgessii* species complex. *Mycologia* 109:935–950

Liu Y, M Wisniewski, JF Kennedy, Y Jiang, J Tang, J Liu (2016). Chitosan and oligochitosan enhance ginger (*Zingiber officinale* Roscoe) resistance to rhizome rot caused by *Fusarium oxysporum* in storage. *Carbohydr Polym* 151:474–479

Lombard L, RV Doorn, PW Crous (2019). Neotypification of *Fusarium chlamydosporum*-a reappraisal of a clinically important species complex. *Fung Syst Evol* 4:183–200

Lombard L, NAVD Merwe, JZ Groenewald, PW Crous (2015). Generic concepts in Nectriaceae. *Stud Mycol* 80:189–245

Nelson PE, TA Toussoun, WFO Marasas (1983). *Fusarium species: An Illustrated Manual for Identification*, pp: 1–191. Pennsylvania State University Press, University Park, Philadelphia, USA

Nirenberg HI, K O'Donnell (1998). New Fusarium species and combinations within the *Gibberella fujikuroi* species complex. *Mycologia* 90:434–458

O'Donnell K, SP McCormick, M Busman, RH Proctor, TJ Ward, G Doehring, DM Geiser, JF Alberts, JP Rheeder (2018). Marasas *et al.* 1984 "Toxigenic Fusarium Species: Identity and Mycotoxicology" revisited. *Mycologia* 27:1058–1080

O'Donnell K, TJ Ward, VARG Robert, PW Crous, DM Geiser, S Kang (2015). DNA sequence-based identification of *Fusarium*: Current status and future directions. *Phytoparasitica* 43:583–595

O'Donnell K, AP Rooney, RH Proctor, DW Brown, SP McCormick, TJ Ward, RJN Frandsen, E Lysøe, SA Rehner, T Aoki, VARG Robert, PW Crous, JZ Groenewald, S Kang, DM Geiser (2013). Phylogenetic analyses of RPB1 and RPB2 support a middle Cretaceous origin for a clade comprising all agriculturally and medically important fusaria. *Fung Gen Biol* 52:20–31

O'Donnell K, DA Sutton, MG Rinaldi, BA Sarver, SA Balajee, HJ Schroers, RC Summerbell, VA Robert, PW Crous, N Zhang, T Aoki, K Jung, J Park, YH Lee, S Kang, B Park, DM Geiser (2010). Internet-accessible DNA sequence database for identifying fusaria from human and animal infections. *J Clin Microbiol* 48:3708–3718

O'Donnell K, DA Sutton, A Fothergill, D McCarthy, MG Rinaldi, ME Brandt, N Zhang, DM Geiser (2008). Molecular phylogenetic diversity, multilocus haplotype nomenclature, and *in vitro* antifungal resistance within the *Fusarium solani* species complex. *J Clin Microbiol* 46:2477–2490

O'Donnell K, BA Sarver, M Brandt, DC Chang, J Noble-Wang, BJ Park, DA Sutton, L Benjamin, M Lindsley, A Padhye, DM Geiser, TJ Ward (2007). Phylogenetic diversity and microsphere array-based genotyping of human pathogenic fusaria, including isolates from the multistate contact lens-associated U.S. keratitis outbreaks of 2005 and 2006. *J Clin Microbiol* 45:2235–2248

O'Donnell K, HC Kistler, E Cigelnik, RC Ploetz (1998). Multiple evolutionary origins of the fungus causing Panama disease of banana: Concordant evidence from nuclear and mitochondrial gene genealogies. *Proc Natl Acad Sci USA* 95:2044–2049

Pérez-Hernández A, Y Serrano-Alonso, MI Aguilar-Pérez, R Gómez-Uroz, J Gómez-Vázquez (2014). Damping-off and root rot of pepper caused by *Fusarium oxysporum* in Almería province, Spain. *Plant Dis* 98:1159

Proctor RH, FV Hove, A Susca, G Stea, M Busman, TVD Lee, C Waalwijk, A Moretti, TJ Ward (2013). Birth, death and horizontal transfer of the fumonisin biosynthetic gene cluster during the evolutionary diversification of *Fusarium*. *Mol Microbiol* 90:290–306

Rojas EC, R Sapkota, B Jensen, HJL Jørgensen, T Henriksson, LN Jørgensen, M Nicolaisen, DB Collinge (2020). Fusarium head blight modifies fungal endophytic communities during infection of wheat spikes. *Microb Ecol* 79:397–408

Ropars J, C Cruaud, S Lacoste, J Dupont (2012). A taxonomic and ecologic overview of cheese fungi. *Intl J Food Microbiol* 155:199–210

Saitou N, M Nei (1987). The neighbor-joining method: A new method for reconstructing phylogenetic trees. *Mol Biol Evol* 4:406–425

Sandoval-Denis M, WJ Swart, PW Crous (2018). New *Fusarium* species from the Kruger National Park, South Africa. *MycoKeys* 34:63–92

Schroers HJ, K O'Donnell, SC Lamprecht, PL Kammeyer, S Johnson, DA Sutton, MG Rinaldi, DM Geiser, RC Summerbell (2009). Taxonomy and phylogeny of the *Fusarium dimerum* species group. *Mycologia* 101:44–70

Snyder WC, HN Hansen (1940). The species concept in *Fusarium*. *Amer J Bot* 27:64–67

Summerell BA (2019). Resolving *Fusarium*: Current Status of the Genus. *Annu Rev Phytopathol* 57:323–339

Tamura K, D Peterson, N Peterson, G Stecher, M Nei, S Kumar (2011). MEGA5: Molecular evolutionary genetics analysis using maximum likelihood, evolutionary distance, and maximum parsimony methods. *Mol Biol Evol* 28:2731–2739

Thompson JD, TJ Gibson, F Plewniak, F Jeanmougin, DG Higgins (1997). The CLUSTAL X windows interface: Flexible strategies for multiple sequence alignment aided by quality analysis tools nucleic acids research. *Nucl Acids Res* 25:4876–4882

Tubaki K, C Booth, T Harada (1976). A new variety of *Fusarium merismoides*. *Trans Braz Mycol Soc* 66:355–366

Tupaki-Sreepurna A, V Thanneru, S Natarajan, S Sharma, A Gopi, M Sundaram, AJ Kindo (2018). Phylogenetic Diversity and *in vitro* susceptibility profiles of human pathogenic members of the *Fusarium fujikuroi* species complex isolated from South India. *Mycopathologia* 183:529–540

Vu D, M Groenewald, MD Vries, T Gehrmann, B Stielow, U Eberhardt, A Al-Hatmi, JZ Groenewald, G Cardinali, J Houbraken, T Boekhout, PW Crous, V Robert, GJM Verkley (2018). Large-scale generation and analysis of filamentous fungal DNA barcodes boosts coverage for kingdom fungi and reveals thresholds for fungal species and higher tax on delimitation. *Stud Mycol* 92:135–154

Wang G, H Chen (1994). The medium for promoting sporulation of *Fusarium*. *Acta Phytopathol Sin* 25:165–166

Wollenweber HW, OA Reinking (1935). *Die Fusarien, ihreBeschreibung, Schadwirkung und Bekämpfung* [M]. Berlin: Paul Parey

Woloshuk CP, WB Shim (2013). Aflatoxins, fumonisins, and trichothecenes: a convergence of knowledge. *FEMS Microbiol Rev* 37:94–109